Nuclear Engineering and Technology 54 (2022) 991–996

Contents lists available at ScienceDirect

Nuclear Engineering and Technology

journal homepage: www.elsevier.com/locate/net

Original article

Radiation damage analysis in SiC microstructure by transmission electron microscopy

Mohd Idzat Idris [a, *], Katsumi Yoshida [b], Toyohiko Yano [b]

[a] The National University of Malaysia, Department of Applied Physics, Faculty of Science and Technology, 43600, Bangi Selangor, Malaysia
[b] Laboratory for Advanced Nuclear Energy, Institute of Innovative Research, Tokyo Institute of Technology, 2-12-1, Ookayama, Meguro-ku, Tokyo, 152-8550, Japan

ARTICLE INFO

Article history:
Received 12 July 2021
Received in revised form
9 September 2021
Accepted 15 September 2021
Available online 16 September 2021

Keywords:
SiC
Neutron irradiation
TEM
Black spot
Dislocation loop
Point defect

ABSTRACT

Microstructures of monolithic high purity SiC and SiC with sintering additives after neutron irradiation to a fluence of 2.0–2.5 × 10^{24} n/m^2 (E > 0.1 MeV) at 333–363 K and after post-irradiation annealing up to 1673 K were observed using a transmission electron microscopy. Results showed that no black spot defects or dislocation loops in SiC grains were found after the neutron irradiation for all of the specimens owing to the moderate fluence at low irradiation temperature. Thus, it is confirmed that these specimens were swelled mostly by the formation of point defects. Black spots and small dislocation loops were discovered only after the annealing process in PureBeta-SiC and CVD-SiC, where the swelling almost diminished. Anomalous-shaped YAG grains were found in SiC ceramics containing sintering additives. These grains contained dense black spots defects and might lose crystallinity after the neutron irradiation, while these defects may annihilate by recrystallization during annealing up to 1673 K. Amorphous grain boundary phase was also presented in this ceramic, and a large part of it was crystallized through post-irradiation annealing and could affect their recovery behavior.

1. Introduction

In the fusion reactor environment, high temperature and radiation fields consist of 14 MeV neutrons, 4 MeV alpha particles, ions and gamma rays become major problems to select excellent materials in order to retain their properties in that severe conditions. From Rovner and Hopkins verified earlier time, the advantages of using low-Z (Z: atomic number) ceramic materials in applying as the first wall and blanket structures in fusion reactors are mentioned several times [1–3]. Therefore, SiC has been proposed as a satisfied candidate material for future components in a nuclear field including fuel cladding material in fission reactors [4]. Besides that, this superior ceramic is able to keep its stability and mechanical strength in fast neutron fluences up to 6.9 × 10^{26} n/m^2 at elevated temperatures [5], which reach up to 1573 K applicable for high-temperature gas-cooled reactors [6].

It is known that cubic SiC has an isotropic expansion when exposed to neutron fluence up to 3 × 10^{24} n/m^2 below 1273 K due to the occurrence of Frenkel defects and black spot defects. Black spot defects are the agglomeration of point defect clusters composed of C and Si interstitials atoms or vacancies with sizes smaller than 2 nm. They are usually found in neutron-irradiated SiC of fluences ≥1 dpa at temperatures ≥873 K. Black spot defects are mostly circular or oval shape, which appeared as nanometer-scale black spots in bright field transmission electron microscopy (TEM) images. This defect contributes to the swelling of the samples, consequently, degrade the material's properties such as significant degradation of mechanical and thermal conductivity. When SiC swelled due to the neutron irradiation followed by mechanical degradation, it will lead to cladding failure and leaking of fission products may occur. Moreover, when thermal conductivity is degraded due to neutron irradiation, the heat produced by the fission reaction is less transferred to the water to generate steam for electric production. In addition, this behavior saturates at a level and slowly decreases with increasing irradiation temperature [7]. Nonetheless, Blackstone and Voice [8] described that the response pattern could change at elevated temperatures, i.e., further swelling has been observed with increasing neutron dose at temperatures about 1173 K and 1473 K in range. It was agreed by Price [6] and Yano et al. [9] that small Frank dislocation loops on {111} planes in pyrolytic β-SiC were observed after neutron-irradiation up to

* Corresponding author.
E-mail address: idzat@ukm.edu.my (M.I. Idris).

https://doi.org/10.1016/j.net.2021.09.015
1738-5733/

12×10^{25} n/m^2 irradiated at 1273 K. Similar report revealed that irradiation at 1523 K and 1723 K will cause continuous expansion of the specimens owing to the tetrahedral void formations [7,10]. Besides, Suzuki et al. [11] summarized that interstitials have agglomerated into dislocations as neutron irradiation proceeds up to 4.8×10^{25} n/m^2. They also estimated that in the experiment, the interstitials were partly released from the interstitial loops and recombine with vacancies or migrate to grain boundary as the neutron-irradiated specimen went through post-irradiation annealing up to 1273 K. Yano et al. confirmed from TEM analysis that the loop size increased and the density decreased by annealing up to 1673 K, supporting the above-mentioned supposition [12].

Previous studies showed that high purity SiC such as PureBeta-SiC and CVD-SiC were swelled approximately 1.24% after the neutron irradiation at fluences of $2.0–2.5 \times 10^{24}$ n/m^2 (E > 0.1 MeV) at 333–363 K owing to the formation of point defects [13]. Further, in the similar report stated that nano-infiltration transient eutectoid (NITE) SiC contained 6 wt% or 9 wt% of alumina and yttria in total as sintering additives were swelled approximately 0.1% more than those of high-purity SiC. The same specimens were annealed in a dilatometer at temperatures of up to 1673 K in order to elucidate their recovery behavior. The results showed that the two types of high-purity SiC and NITE-SiC specimen contained 12 wt% alumina, yttria and silica were recovered completely after annealing at 1573 K. However, another NITE-SiC specimen contained 18 wt% of similar sintering additives was not recovered fully to pre-irradiation length [14,15]. Apparently, neutron-irradiation induced point defects in SiC could be annihilated through recombination by post-irradiation annealing, thus stimulate a volume contraction (recovery).

The purposes of this study are to evaluate the microstructure of high purity SiC and SiC with sintering additives by transmission electron microscopy (TEM) after neutron irradiation with intermediate fluence at relatively low temperatures. Further, the microstructure of irradiated specimens that recovered well through a heat treatment has been observed to clarify the microstructure evolution. Besides, the effects of the secondary phase on the microstructure of SiC after neutron irradiation and post-irradiation annealing were examined and compared to those of high purity SiC.

2. Experimental procedures

2.1. Materials

High purity, i.e., almost no metallic impurities, β-SiC polycrystals, PureBeta-SiC (Bridgestone, Japan) and CVD-SiC (Rohm and Haas Advanced Materials, USA) were used. Pure β-SiC is made by hot press sintering with non-metal agents in vacuum conditions at ≤1673 K or in the inert gas atmosphere at ≤1973 K to ensure high purity. In addition, it contained a small amount of carbon inclusions at grain boundaries. Pure β-SiC and CVD-SiC have a full density of approximately 3.14 g/cm^3 and 3.21 g/cm^3, respectively. Furthermore, SiC that contained either 12 wt% or 18 wt% of alumina, silica, and yttria as sintering additives (Kyoto Univ. Japan) were applied in this study. Descriptions of each specimen were mentioned elsewhere [14,15]. Specimens were simultaneously neutron-irradiated in the BR2 reactor of SCK·CEN (Belgium) at fluences of $2.0–2.5 \times 10^{24}$ n/m^2 (E > 0.1 MeV, 0.20–0.25 dpa). The irradiation temperature of the specimens was 333–363 K and the duration of irradiation was 60 days. For post-irradiation annealing experiments, irradiated specimens from both types of SiC were annealed from room temperature to 1673 K, in a step-wise manner at intervals of 50 K and were kept for 6 h at each step. The same procedures were applied for not only SiC [15–17] and AlN [18] but also for Si_3N_4 [19] or graphite [20]. Then, each of the specimens with different conditions (unirradiated, irradiated, and post-irradiation annealed) was observed by TEM. Based on the results of post-neutron-irradiation annealing, Pure β-SiC and CVD-SiC showed similar recovery behavior for closely positioned C and Si Frenkel pairs. Their activation energies have four stages which are in the range of 0.12–0.24 eV, 0.002–0.04 eV, 0.20–0.31 eV, and 1.26–1.38 eV at various temperatures.

2.2. Specimen preparation and TEM observation

The unirradiated and irradiated specimens were cut into half using a diamond saw. The dimensions of the resulting halves were 25 mm × 1.5 mm × 2 mm and each half was used in annealing experiment and TEM observation. Next, half of the TEM specimen was cut into several slices with a thickness of approximately 400 μm. Each slice was thinned until the thickness becomes nearly 100 μm using a 20 μm grinder disk. The grinded specimen was dimpled at the center using a grinder (Model 656 N, GATAN), together with diamond slurry (3–4 μm). Afterward, the specimen was placed in molybdenum (Mo) double mesh, which had cut in the center for the ion milling process using an Atom Beam Thinning Apparatus (Model 806A, UK) with 7 kV acceleration voltage and 1 mA of beam current in a vacuum. The ion beams derived from Ar gas were directed from lower and upper guns with a glancing angle of 20°. After a hole emerged, the specimen was coated by carbon using a Sputter Coater (Model SC500, Meiwa) to prevent charging during observation.

The transmission electron microscope used in this study was the Hitachi H-9000 instrument at an accelerating voltage of 300 kV with a filament current of 8 μA. Point to point resolution of this microscope is 0.20 nm. Further, high-resolution electron microscopy (HREM) technique was used to observe the atomic configuration of each specimen without any objective aperture.

3. Results and discussion

3.1. PureBeta SiC

Fig. 1 shows several TEM images of the PureBeta-SiC specimen. (a, b) represents the unirradiated specimen, (c, d) represents the irradiated specimen, and (e, f) presents the post-irradiation annealed specimen up to 1673 K. Images were taken with low and high magnifications. A few grains without pores, precipitates, or dislocation loops can be seen in the unirradiated specimen (Fig. 1 (a)) with an average size of approximately 3–4 μm. Several stacking faults were observed as shown in Fig. 1 (b), and these stacking faults in SiC generally exist in cubic dense-packed {111} planes [12]. In the case of the irradiated PureBeta SiC, no black spot defects or dislocation loops are visible as shown in Fig. 1 (c) and (d). It is suggested that, due to moderate fluence at low irradiation temperature, swelling of SiC contributed mostly by point defects [17]. Fig. 1 (e) and (f) show the microstructure of the irradiated PureBeta SiC after the heat treatment up to 1473 K. The figures explicitly show that a few nm of black spots distribute throughout SiC grains. It is noted at this condition, the macroscopic length of the irradiated PureBeta SiC almost recovered to the similar length of the unirradiated specimen via recombination of interstitial atoms and vacancies through the annealing process up to 1673 K.

It was reported that interstitials of these irradiated specimens started to recombine with vacancies at above 363 K, similar to the irradiation temperature [14,15]. As annealing temperature increases, the recombination proceeds gradually, and finally macroscopic length of the irradiated specimen reaches the pre-irradiation length. It is known that the number of interstitial atoms equal with that of vacancies due to the generation of Frenkel pairs by neutron

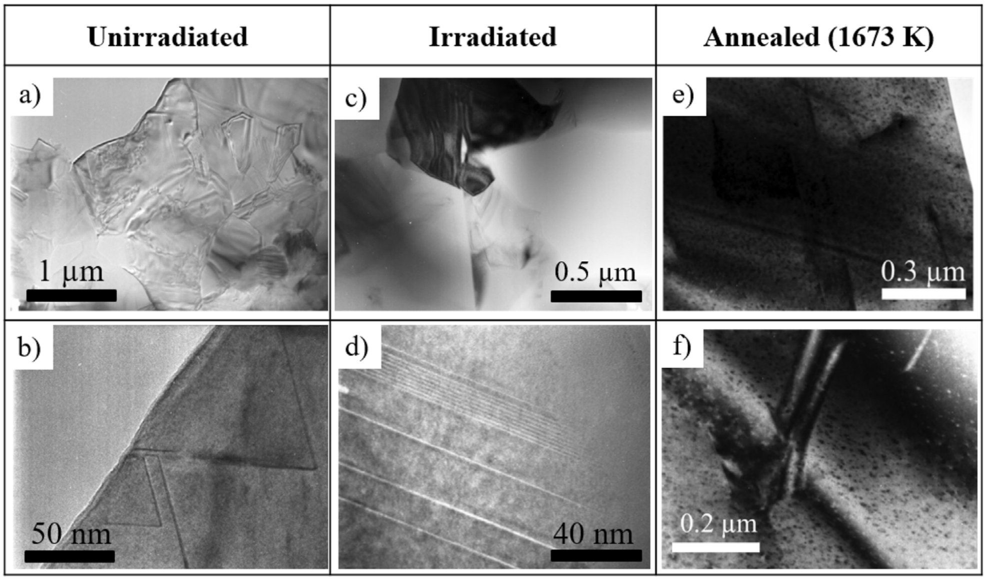

Fig. 1. Microstructures of unirradiated, irradiated and post-irradiation annealed PureBeta SiC. Fig. a) shows a few grains with an average size of approximately 3–4 μm, while several stacking faults were observed in Fig b). The irradiated sample shows no black spot defects or dislocation loops are visible as shown in Fig. c) and d). However, significant numbers of black spots have been observed after the annealing process (e, f).

irradiation. In general, Frenkel defects remaining in a crystal after irradiation cause swelling of a ceramic material. Frenkel defects will recombine each other with a similar number due to annealing, where it leads to volume contraction. A study showed that recombination of point defects mostly occurs below 1473 K [21]. Nearly three-fourth of recovery occurred by recombination for closely positioned C and Si Frenkel pairs less than 1223 K. Beyond that temperature, recombination of slightly separated C Frenkel pairs and more long-range migration of Si interstitials could be occurred gradually and lead to lattice contraction [14]. Essentially, under annealing technique interstitials tend to recombine with vacancies and finally, defects are annihilated. However, specimens irradiated under some conditions, the surviving interstitials/very small clusters tend to coagulate with other interstitials and form interstitial clusters or interstitial dislocation loops during the recombination process, particularly at temperatures higher than 1273 K [12,22,23]. Fig. 1 (e, f) indicates the growth of defects by annealing.

Fig. 2a) and b) shows high-resolution micrographs of unirradiated and irradiated PureBeta SiC, respectively, and was taken with [110] beam direction corresponds to the selected area diffraction patterns as inserted in the figure. These diffraction patterns clarify that all observed grains have a cubic structure, which was maintained after the neutron irradiation. Small dots on the figure correlate with the tetrahedron of SiC [9]. Both of the irradiated and unirradiated specimens' high-resolution micrographs have a mostly perfect crystalline arrangement with a normal lattice of β-SiC, and no interstitial dislocation loops were found in these photographs. However, only the stacking sequences change owing to stacking faults lying on the {111} planes were observed, as indicated with lines in the photographs. According to Yano et al. [21], if small defect clusters of 1 nm in size exist, the high-resolution image has many patches of dark or bright contrast in the background with a curved array of lattice fringes. Meanwhile, defects larger than 1 nm in the periodic lattice should be visible under high-resolution electron microscopy. Therefore, Fig. 2 further supports that the

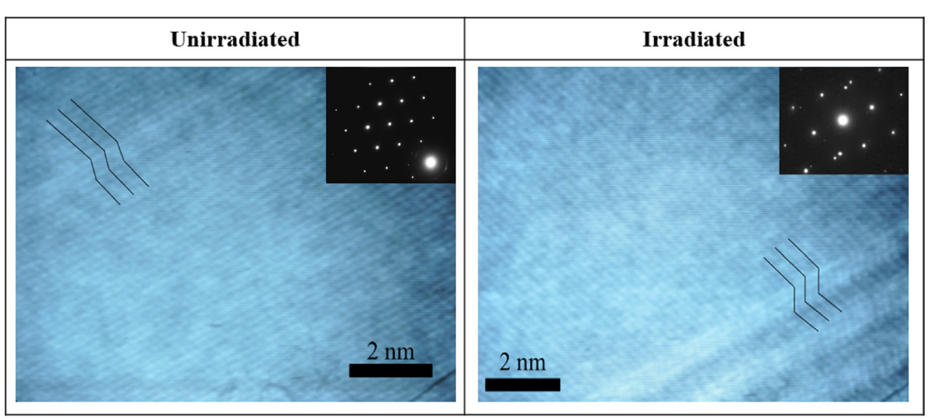

Fig. 2. High-resolution micrographs of a) unirradiated and b) irradiated PureBeta SiC were taken with [110] beam direction. The irradiated sample has a perfect crystalline arrangement with a normal lattice of PureBeta SiC with no interstitial loops were found, similar to an unirradiated sample. Only the stacking sequences change owing to stacking faults lying on the {111} planes were observed.

neutron-irradiated induced swelling is mostly originated from point defects in PureBeta SiC.

3.2. CVD-SiC

Fig. 3 depicts bright-field images of the CVD-SiC specimens; unirradiated (a, b), irradiated (c, d) and post-irradiation annealed up to 1673 K (e, f). Average grain size is 5–6 μm and several initial stacking faults lying on the {111} planes similar to PureBeta SiC are observed in the unirradiated specimen. Senor et al. [23] reported that unirradiated CVD-SiC has a columnar grain structure in <111> CVD growth direction and the faulted microstructure without porosity or precipitates. The microstructure of the irradiated CVD-SiC is similar to the irradiated PureBeta SiC, where there are no black spot defects or dislocation loop have been found. An only highly faulted area with common stacking faults of a few 100 nm has been observed. Katoh et al. [24] reported that CVD-SiC exposed to neutron fluence of 6.0 $\times$ 10^{25} n/m^2 at 573 K has small clusters with a strain contrast and were identified as black spot defects. Further, the volumetric average swelling by cavities in the specimen is estimated to be <1% when exposed with 100 dpa at 1673 K. Besides, the evolution of interstitials loops has been reported to occur between 753 K and 793 K if irradiated at 2.8 $\times$ 10^{26} n/m^2 [25]. Snead et al. [7] summarized the growth of black spot defects, dislocation loops, and voids, where it could be deduced that small clusters emerge as black spot defects evolve into dislocation loops and eventually form voids when neutron fluence increases and irradiation temperature is high. Hence, swelling induced by neutron irradiation in the present CVD-SiC specimen is mainly caused by Frenkel defects, similar to the PureBeta SiC specimen.

It is known that present irradiated CVD-SiC underwent almost complete recovery by the post-irradiation annealing up to 1673 K [14]. However, a perceptible occurrence of black spots is distributed throughout the grain after annealing at 1673 K as shown in Fig. 3 (e). The size is slightly larger than the black spots in PureBeta SiC. Furthermore, red circles in Fig. 3 (f) indicate small dislocation loops with 9 nm in diameter parallel with the stacking faults lying on the {111} planes. Numerous studies have observed dislocation loops in CVD-SiC after neutron-irradiated at high neutron fluences or elevated irradiation temperatures. For instance, Kondo et al. [26] asserted that relatively large loops with 6.3 nm in radius were visible after the neutron irradiation of 5.3 $\times$ 10^{25} n/m^2 irradiated at 1573 K. Another report stated that dislocation loops around 10–20 nm were observed on the {111} planes after irradiated to 28 and 37 dpa at 753 and 858 K, respectively [9]. However, in this study, neither black spots nor dislocation loops were found in the as-irradiated specimen, but they were discovered after the post-irradiation annealing, where the swelling was almost diminished. Hence, the black spots or dislocation loops are not the main factors of swelling induced by neutron irradiation. They are likely starting to grow at around 873 K below 1 dpa [7]. Similar to PureBeta SiC, during recombination process surviving interstitials that not annealed out were inclined to agglomerate and form black spots defects or dislocation loops. In addition, CVD-SiC has lower activation energies for length shrinkage than that of PureBeta SiC at 1323–1523 K [14]. This result showed that the remained interstitials in irradiated CVD-SiC are easier to gather by themselves particularly at elevated temperatures. Therefore, slightly large black spots and small dislocation loops can be observed by TEM in CVD-SiC after the heat treatment. It can be concluded that these black spots and/or dislocation loops that appeared in the microstructure of high purity SiC are not the defects induced directly by the neutron irradiation. It is confirmed that only Frenkel defects are the dominant feature in both specimens after mild neutron fluence at low irradiation temperature.

No formation of voids was found even irradiated PureBeta SiC and CVD-SiC were annealed up to 1673 K. It has been reported that void starts to grow during neutron irradiation at 1403 K or 1523 K [6,7]. Very sparse cavities have been observed in highly twined or faulted grains in SiC after irradiation up to 7.7 $\times$ 10^{25} n/m^2 at 1403 K [26]. The similar report revealed that small cavities in a spherical shape and faceted voids are formed after exposed to 1.9 $\times$ 10^{25} n/m^2 at 1733 K. The volume and the shape of the voids were increased and change to triangular or hexagonal as fluence increases up to

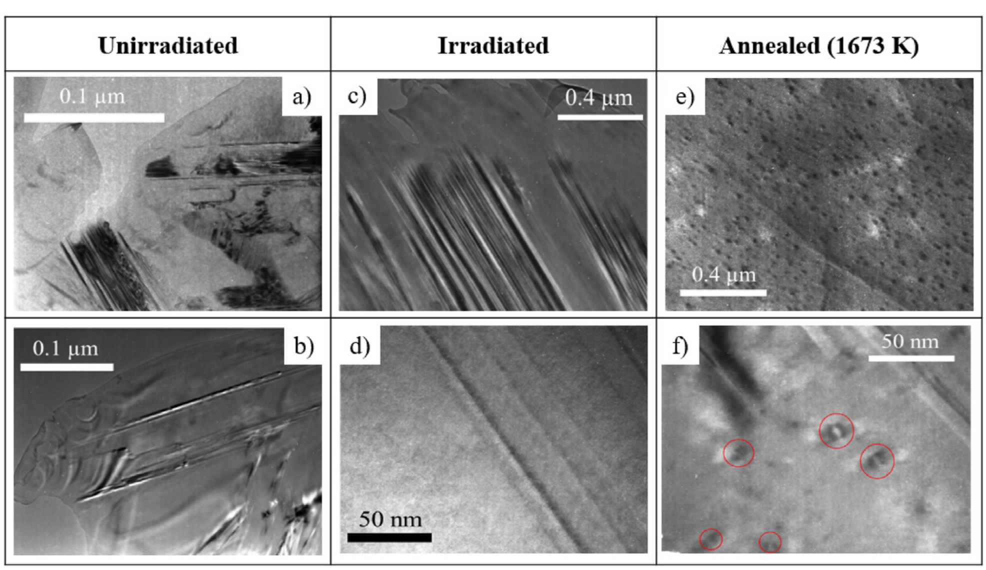

Fig. 3. Microstructures of unirradiated, irradiated and post-irradiation annealed CVD-SiC. The average grain size is 5–6 μm and several initial stacking faults lying on the {111} planes as shown in Fig a) and b). There are no black spot defects or dislocation loop that have been found in the irradiated sample as shown in Fig c) and d). However, Fig e) shows black spots are distributed throughout the grain, while red circles in Fig. (f) indicate small dislocation loops with 9 nm in diameter found in the annealed sample. (For interpretation of the references to colour in this figure legend, the reader is referred to the Web version of this article.)

9.6×10^{25} n/m^2. Irradiation conditions of the present specimens are much less fluence and lower irradiation temperature than those previous conditions mentioned above so that it is reasonable that cavities were not to be observed.

3.3. NITE-SiC

Fig. 4 shows microstructures of SiC with 12 wt% (NITE-A) and 18 wt% (NITE-B) of sintering additives; unirradiated (a, b), irradiated (c, d) and post-irradiation annealed up to 1673 K (e, f). Significantly, NITE-A has a larger grain size (250 nm) than NITE-B (130 nm) on average owing to the less amount of sintering additives. Further, crystalline YAG has been identified as large irregular-shaped grains without stacking fault. It is noted that the crystalline YAG phase was only detected by XRD in unirradiated NITE specimens [13]. A bright and lacy-contrasted phase is supposed as an oxide glassy phase which embedded partly at the triple junction and as the continuous phase, as shown in Fig. 4 (a) and (b), respectively. Elements related to the additives were not detected inside SiC grains for both specimens. The microstructure of the unirradiated NITE-B specimen shows that a large area is covered by a continuous oxide glassy phase compared to the unirradiated NITE-A specimen. According to Park et al. [27], NITE-SiC had an appreciably fine mean size of the grain, while oxide glassy phase was observed at the grain boundary and the triple junction because it was manufactured at low temperature (2073 K) with the heating period of less than 1 h. Another report stated that the glassy phase has been identified in NITE-SiC as a secondary phase and 90% of them were YAG located at the triple junction [28]. Features of the present NITE specimens have well coincided with these reports.

Investigations on microstructures of the irradiated NITE A and B specimens revealed that there are anomalous-shaped YAG grains with inhomogeneous and dark-contrasted, as shown in Fig. 4 (c) and (d). There is a limited reference regarding the irradiation effects on monolithic YAG, particularly on its microstructure. However, it could be suggested that the inhomogeneous and dark contrast of YAG grains indicates it contains high-density black spot defects that have been observed in heavily irradiated SiC. Further, a small number of amorphous YAG was recrystallized by neutron irradiation as an irregular shape. Konishi et al. [29] reported that the crystallinity of monolithic YAG is reduced significantly after the neutron irradiation of the same conditions that performed in this study, hence induced large swelling. Additionally, monolithic YAG were swelled 0.5% and 0.2% after severe neutron-irradiation of a fluence of 4.6×10^{25} n/m^2 at 710 K and 2.8×10^{25} n/m^2 at 1015 K, respectively, and would generate edge type dislocations [30,31]. A report explained that no resolvable defect aggregates in monolithic YAG after neutron irradiation up to 2×10^{25} n/m^2 at 925 K and 0.3×10^{25} n/m^2 at 1015 K. Only a sparse formation of faulted {110} dislocation loops was observed after exposure to a higher irradiation temperature above 1100 K [32]. Therefore, it is reasonable that YAG grains containing high-density black spot defects and probably loose crystallinity under the present irradiation condition [29].

Microstructures of irradiated NITE-A and NITE-B after the annealing process are shown in Fig. 4 (e) and (f), respectively. Contrary to the PureBeta SiC and CVD-SiC specimens, no black spots or dislocation loops were observed in SiC grains. However, it is not clear why black dots defects were not observed in SiC grains of NITE specimens after the same annealing, whereas they were observed in PureBeta and CVD-SiC. It is noted that NITE A was shrunk slightly and NITE-B was not recovered fully (~0.2% greater than the pre-irradiation length) after the heat treatment up to 1673 K. Since both of them have sintering additives, this means that the oxide grain boundary phases or secondary phases, which are probably crystallized during the fabrication process or the annealing process, are additional factors affecting the recovery behavior of irradiated NITE specimens. Therefore, it also affected the occurrence of black spot defects. It is assumed that in NITE-A and NITE-B, no agglomeration of C and Si Frenkel pairs were happened as in the Pure β-SiC and CVD-SiC. The activation energies obtained from the annealing process are for the only recombination of point defects of C and Si, and crystallization of sintering additives elements.

Only slightly darker-contrasted grains were observed as shown in Fig. 4 (c, d), corresponding to YAG grains. Note that the contrast of YAG grains change greatly when inclining and it showed electron diffraction patterns. Determination of activation energy showed that length recovery occurred mostly by recombination of close interstitial atoms and vacancies through the annealing process. At

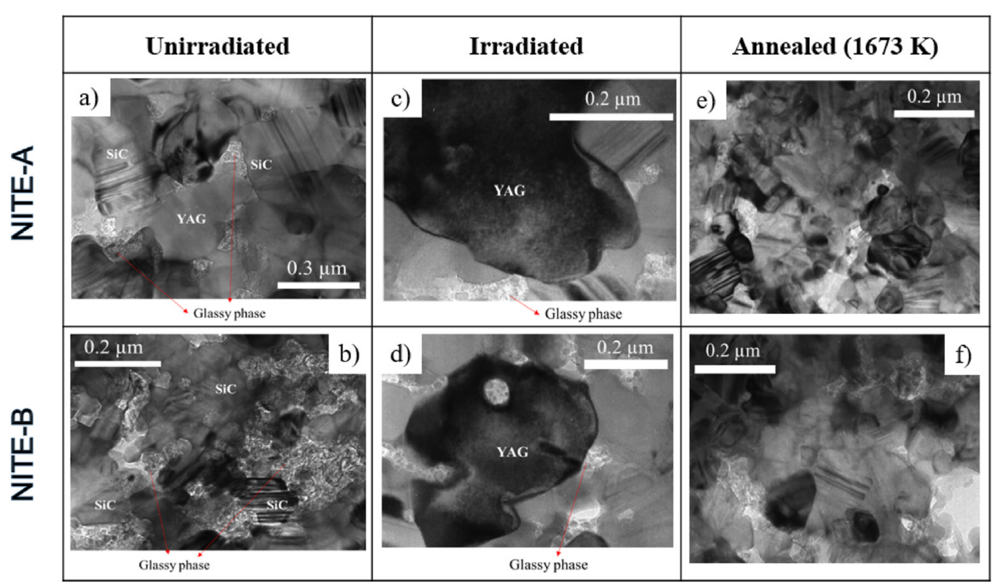

Fig. 4. Microstructures of unirradiated, irradiated and post-irradiation annealed NITE-A and NITE-B. a) and b) show occurrence of oxide glassy phase (YAG). c) and d) show an inhomogeneous contrast and an anomalous shape of YAG grains, respectively. e) and f) show less amount of amorphous YAG phase due to recrystallization via post-irradiation annealing.

the same time, amorphized YAG was recrystallized more significantly than before irradiation [15]. It is supposed that defects induced into YAG crystal grains may annihilate during recrystallization. It is seemly less amount of the amorphous YAG was observed for both specimens after annealing as shown in Figure e) and f). Up to now, very limited data has been shown regarding post-irradiation annealing treatment on YAG. It is noted that NITE-B did not recover completely since the amorphous YAG formed as the continuous phase [15]. Thus, it could affect the whole properties of NITE-B including its recovery behavior. In the case of NITE-A, it exhibits similar responses as high purity SiC during post-irradiation annealing up to 1523 K owing to the less amount of amorphous YAG phase that formed partly at the triple junction.

4. Conclusions

The microstructure of unirradiated, neutron-irradiated and post-irradiation annealed PureBeta SiC, CVD-SiC, NITE-A, and NITE-B SiC ceramics were investigated by transmission electron microscopy. Further, high-resolution electron microscopy (HREM) technique was used to observed atomic configuration in PureBeta-SiC and CVD-SiC. The results were summarized as follows;

1. Black spot defects or dislocation loops in high purity SiC and SiC with sintering additives were not observed by TEM after irradiation with mild neutron fluence at low irradiation temperature (2.0–2.5 × 10^{24} n/m^2 (E > 0.1 MeV) at 333–363 K).
2. It is suggested that the swelling occurred mostly due to the formation of point defects.
3. Black spots and small dislocation loops were observed in both high purity SiC after post-irradiation annealing up to 1673 K due to coagulation of interstitials that did not annihilate out.
4. Anomalous-shaped YAG grains were found in SiC containing sintering additives. These crystals containing dense black spots defects and my loose crystallinity after the neutron irradiation, while these defects may annihilate by recrystallization during annealing up to 1673 K. Amorphous grain boundary phase were also presented in this ceramic, and a large part of it was crystallized through post-irradiation annealing and could affect their recovery behavior.

Declaration of competing interest

The authors declare that they have no known competing financial interests or personal relationships that could have appeared to influence the work reported in this paper.

Acknowledgments

The study was partly supported by a university's grant (GUP-2018-154 and KRA-2018-057) and by the Japan Atomic Energy Agency through ITER-BA activity. The irradiation experiments were performed with support from the staff of the International Research Center for Nuclear Materials Science, Institute for Materials Research, Tohoku University.

References

[1] L.H. Rovner, G.H. Hopkins, Ceramic materials for fusion, Nucl. Technol. 29 (1976) 274.
[2] G.P. Pells, Ceramic materials for fusion reactor applications, J. Nucl. Mater. 122&123 (1984) 1338.
[3] H. Bolt, Nonmetallic materials for plasma facing and structural applications in fusion reactors, Fusion Eng. Des. 22 (1993) 85.
[4] K. Ahn, K. Joo, S. Park, Safety evaluation of silicon carbide and zircaloy-4 cladding during a large-break loss-of-coolant accident, Energies 11 (2018) 3324.
[5] M. Akiyoshi, T. Yano, Neutron-irradiation effect in ceramic evaluated from macroscopic property changes in as-irradiated and annealed specimens, Prog. Nucl. Energy 50 (2008) 567.
[6] R.J. Price, Neutron irradiation-induced voids in β-silicon carbide, J. Nucl. Mater. 48 (1973) 47.
[7] L.L. Snead, T. Nozawa, Y. Katoh, T. Byun, S. Kondo, D.A. Petti, Handbook of SiC properties for fuel performance modelling, J. Nucl. Mater. 371 (2007) 329.
[8] R. Blackstone, E.H. Voice, The expansion of silicon carbide by neutron irradiation at high temperature, J. Nucl. Mater. 39 (1972) 319.
[9] T. Yano, T. Iseki, High-resolution electron microscopy of neutron-irradiation-induced dislocations in SiC, Phil. Mag. 62 (1990) 421.
[10] S. Kondo, Y. Katoh, L.L. Snead, Cavity swelling and dislocation evolution in SiC at very high temperatures, J. Nucl. Mater. 386–388 (2009) 222.
[11] T. Suzuki, T. Maruyama, T. Iseki, T. Mori, M. Ito, Recovery behavior in neutron irradiated β-sic, J. Nucl. Mater. 149 (1987) 334.
[12] T. Yano, T. suzuki, T. Maruyama, T. Iseki, Microstructure and annealing behavior of heavily neutron-irradiated β-SiC, J. Nucl. Mater. 155–157 (1988) 311.
[13] M.I. Idris, S. Yamazaki, K. Yoshida, T. Yano, Defects annihilation behavior of neutron-irradiated SiC ceramics densified by liquid-phase-assisted method after post-irradiation annealing, J. Nucl. Mater. Energy. 9 (2016) 199.
[14] M.I. Idris, H. Konishi, M. Imai, K. Yoshida, T. Yano, Neutron irradiation swelling of SiC and SiCf/SiC for advanced nuclear applications, Energy Procedia 71 (2015) 328.
[15] M.I. Idris, S. Yamazaki, K. Yoshida, T. Yano, Recovery behavior of high purity cubic SiC polycrystals by post-irradiation annealing up to 1673 K after low temperature neutron irradiation, J. Nucl. Mater. 465 (2015) 814.
[16] S. Yamazaki, M. Imai, T. Yano, Recovery of neutron-induced damage of SiC by thermal annealing up to 1400 °C, Prog. Nucl. Energy 50 (2008) 601.
[17] T. Yano, Y. You, K. Kanazawa, T. Kobayashi, M. Imai, K. Yoshida, S. Yamazaki, Recovery behavior of neutron-irradiation-induced point defects of high-purity β-SiC, J. Nucl. Mater. 455 (2014) 445.
[18] T. Pornphatdetaudom, T. Yano, K. Yoshida, Physical property changes of neutron-irradiated aluminum nitride and their recovery behavior by annealing using a step-heating dilatometer, Nucl. Mater. Energy. 16 (2018) 24.
[19] A. Rueanngoen, K. Kanazawa, M. Imai, K. Yoshida, T. Yano, Analysis of recovery process of low-dose neutron irradiation-induced defects in silicon nitride-based ceramics by thermal annealing, J. Nucl. Mater. 455 (2014) 464.
[20] Y. Jin, K. Yoshida, Z. Li, D. Ai, T. Maruyama, T. Yano, Investigation of kinetic recovery process in low dose neutron-irradiated nuclear graphite by thermal annealing, J. Nucl. Sci. Technol. 56 (2019) 533.
[21] T. Yano, H. Miyazaki, M. Akiyoshi, T. Iseki, X-ray diffractometry and high-resolution electron microscopy of neutron-irradiated SiC to a fluence of 1.9×10^{27} n/m^2, J. Nucl. Mater. 253 (1998) 78.
[22] T. Yano, B. Matovic, Handbook of Advanced Ceramics: Advanced Ceramics for Nuclear Applications, Academic Press, USA, 2013, p. 353.
[23] D.J. Senor, G.E. Youngblood, L.R. Greenwood, D.V. Archer, D.L. Alexander, M.C. Chen, G.A. Newsome, Defect structure and evolution in silicon carbide irradiated to 1 dpa-SiC at 1100 °C, J. Nucl. Mater. 317 (2003) 145.
[24] Y. Katoh, N. Hashimoto, S. Kondo, L.L. Snead, A. Kohyama, Microstructural development in cubic silicon carbide during irradiation at elevated temperatures, J. Nucl. Mater. 351 (2006) 228.
[25] T. Yano, M. Akiyoshi, K. Ichikawa, Y. Tachi, T. Iseki, Physical property change of heavily neutron-irradiated Si_3N_4 and SiC by thermal annealing, J. Nucl. Mater. 289 (2001) 102.
[26] S. Kondo, Y. Katoh, L.L. Snead, Microstructural defects in SiC neutron irradiated at very high temperatures, J. Nucl. Mater. 382 (2008) 160.
[27] J.S. Park, Y. Katoh, A. Kohyama, J.K. Lee, J.J. Sha, H.K. Yoon, Tailoring the microstructure of hot-pressed SiC by heat treatment, J. Nucl. Mater. 329–333 (2004) 558.
[28] T. Koyanagi, Microstructural analysis of secondary phases in silicon carbide fabricated with SiC nano-powder and sintering additive, Ceram. Mater. Energy App. 32 (2011) 53.
[29] H. Konishi, M.I. Idris, M. Imai, K. Yoshida, T. Yano, Neutron irradiation effects of oxide sintering additives for SiCf/SiC composites, Energy Procedia 71 (2015) 306.
[30] R.J.M. Konings, K. Bakker, J.G. Boshoven, R. Conrad, H. Hein, The influence of neutron irradiation on the microstructure of Al_2O_3, $MgAl_2O_4$, $Y_3Al_5O_{12}$ and CeO_2, J. Nucl. Mater. 254 (1998) 135.
[31] G.F. Hurley, J.M. Bunch, Swelling and thermal diffusivity changes in neutron-irradiated ceramics, Am. Ceram. Soc. Bull. 59 (1980) 456.
[32] F.W. Clinard Jr., G.F. Hurley, R.A. Youngman, L.W. Hobbs, The effect of elevated-temperature neutron irradiation on fracture toughness of ceramics, J. Nucl. Mater. 133&134 (1985) 701.